

# Nuclear effects and their interplay in nuclear DVCS amplitudes

A. Freund

*Institut für Theoretische Physik, Universität Regensburg, D-93040 Regensburg, Germany*

M. Strikman

*Department of Physics, The Pennsylvania State University,  
University Park, PA 16802, USA*

In this paper we analyze nuclear medium effects on DVCS amplitudes in the  $x_{bj}$  range of  $10^{-1} - 10^{-4}$  for a large range of  $Q^2$  and four different nuclei. We use our nucleon GPD model capable of describing all currently available DVCS data on the proton and extend it to the nuclear case using two competing parameterizations of nuclear effects. The two parameterizations, though giving different absolute numbers, yield the same type and magnitude of effects for the imaginary and real part of the nuclear DVCS amplitude. The imaginary part shows stronger nuclear shadowing effects compared to the inclusive case i.e.  $F_2^N$ , whereas in the real part nuclear shadowing at small  $x_{bj}$  and anti-shadowing at large  $x_{bj}$  combine through evolution to yield an even greater suppression than in the imaginary part up to large values of  $x_{bj}$ . This is the first time that such a combination of nuclear effects has been observed in a hadronic amplitude. The experimental implications will be discussed in a subsequent publication.

PACS numbers: 11.10.Hi, 11.30.Ly, 12.38.Bx

## I. INTRODUCTION

Currently information about parton structure of nuclei is very limited. Most of the data were obtained at rather large  $x_{bj} \geq 5 \times 10^{-2}$  where deviations of the nuclear structure from additivity for  $F_{2A}$  are of the order of a few percent, until one reaches the region of the EMC effect  $x_{bj} \geq 0.4$  where the structure functions themselves are already pretty small. For gluons the situation is even more uncertain - the theoretical analysis based on QCD momentum sum rules and the expectation of a significant nuclear shadowing [1, 2] leads one to expect a gluon enhancement of the order of 10 – 20% for  $x_{bj} \sim 0.1$ . The analysis of the NMC data supports such a conclusion [3, 4]. However, the  $Q^2$  range of the NMC data is rather limited and higher twist effects may affect the analysis substantially.

The interpretation of the data at smaller  $x_{bj}$  where one observes the shadowing of  $F_{2A}$ , is even more difficult. This is due to the strong correlation of  $x_{bj}$  and  $Q^2$  in the relevant kinematic region of  $x_{bj} \leq 10^{-2}$ ,  $Q^2 \leq 2 \text{ GeV}^2$ . In this kinematic region theoretical calculations of shadowing based on the Gribov theory connecting diffraction in eN scattering and shadowing in eA scattering describe the data well. However, in these analysis the vector meson contribution which is a higher twist effect was found to be substantial thus indicating the importance of higher twist shadowing effects [5, 6, 7]. In principle, local duality could result in the vector meson contribution being dual to the continuum. However, the recent analysis in [8] based on the theory of leading twist nuclear parton shadowing [9, 10] has explicitly demonstrated that 30 – 40% of the shadowing for  $F_{2A}(x_{bj} \leq 10^{-2}, Q^2 \leq 2 \text{ GeV}^2)$  is due to higher twist effects.

Clearly in this situation one needs new experimen-

tal tools to study the nuclear partonic structure. Exclusive reactions appear to be a very natural candidate. Among them deeply virtual Compton scattering (DVCS) (see Fig. 1) is the simplest reaction since the final state real photon cannot be involved in the rescatterings, while in the case of meson production a suppression of final state interactions (color transparency) probably requires rather large values of  $Q^2$ .

The most interesting production channel to investigate is the one where the nucleus remains intact - coherent nuclear DVCS. The generalized parton distributions (GPDs) which enter in this case carry much more direct information about the nuclear structure than the channels with a nuclear break-up. Besides, the extraction of the coherent signal is much easier experimentally both for fixed target experiments with relatively modest resolution on the missing mass, and for future collider experiments like the planned Electron Ion Collider (EIC) where it will be possible to use a zero angle calorimeter to select events where the nucleus remained intact.

This, however, comes at a price. The average values of  $t$  in the coherent scattering are small  $\sim 3/R_A^2$  and can hardly be measured. Hence, one has to deal with cross sections integrated over  $t$ . The challenge in this case will be to observe the DVCS signal at small  $t$  and small  $x_{bj}$  where the QED Compton or Bethe-Heitler process is very important.

Thus our task in studying nuclear DVCS is two fold. First, we want to construct generalized nuclear parton distribution functions relevant for the discussed process and then to calculate the DVCS amplitudes beyond the impulse approximation which was considered in [11] for both coherent and incoherent channels. This will be the subject of the first of two papers. In the second paper we will study various DVCS observables to find out which of them are feasible for small  $x_{bj}$  DVCS studies.

Our strategy will be to combine techniques which we developed in the modeling of next-to-leading order

(NLO) GPDs for nucleons in [12] and which describe the current world DVCS data [13] with fairly high accuracy and the recent calculations of nuclear PDFs at small  $x_{bj}$  [8, 9, 10]. These calculations are based on the connection between diffractive parton densities measured at HERA and shadowing for nuclear parton densities [9] and indicate that at small  $x_{bj}$  shadowing should be large in both the quark and gluon channels.

There are several aspects of nuclear DVCS at small  $x_{bj}$  which appear interesting. One goal would be to test our understanding of the connection between PDFs and GPDs. Qualitatively, we expect that the shadowing regime will start for the imaginary part of DVCS at larger  $x_{bj}$  since the effective  $x_{bj}$  which enters in the DVCS amplitudes is of the order of  $x_{bj}/2$ . The space-time picture of DVCS points in the same direction since the coherence length in the transition of an intermediate state of mass,  $M$ , into a real photon is larger than in the case of DIS - the non-covariant propagator is  $\sim 1/M^2$  instead of  $1/(M^2 + Q^2)$ . Another aspect is the importance of the gluon GPD feeding into the quark singlet GPD in the course of evolution especially in the NLO approximation which was demonstrated in [14]. Since the shadowing of gluons and quarks turns out to be different within the model adopted in this paper, we expect the A-dependence of the DVCS observables to be different from that of  $F_{2A}$ . For a comparison we will give also results based on the model of [4] which is based on a fit to  $x_{bj} \geq 10^{-2}$  data assuming leading twist dominance and extrapolating to smaller  $x_{bj}$  with the assumption that the gluon and quark parton densities are screened in the same way at the initial scale of perturbative QCD evolution. Another unique aspect of DVCS is the ability to measure the real part of the amplitude. In this case we expect significant nuclear effects already at rather large  $x_{bj} \simeq 0.1$  since the real part of the DVCS amplitude is sensitive to the rate of variation of parton densities with  $x_{bj}$ , which, for the nuclear case, is already rather different at  $x_{bj} \sim 5 \times 10^{-2}$ .

Studies of nuclear DVCS will have important spin offs for studies of color transparency in coherent high energy reactions since the same GPDs enter in both DVCS and vector meson production. Hence comparing results for these two processes will allow one to find the value of  $Q^2$  at which perturbative color transparency becomes essentially model independent.

This paper is organized as follows: In section II we summarize the procedure for modeling nuclear GPDs based on the information about nucleon GPDs. We will also discuss the accuracy of factorizing GPDs as a product of the GPD at  $t = 0$  and the nuclear form factor.

In the next section we summarize the previous findings on NLO DVCS amplitudes and give numerical results for a set of nuclei. We will demonstrate that nuclear effects are indeed quite strong and different from the case of  $F_{2A}$ . We find that there is a significant difference between nuclear effects between the two cases. Interestingly enough we find that the nuclear effects for the real part of the am-

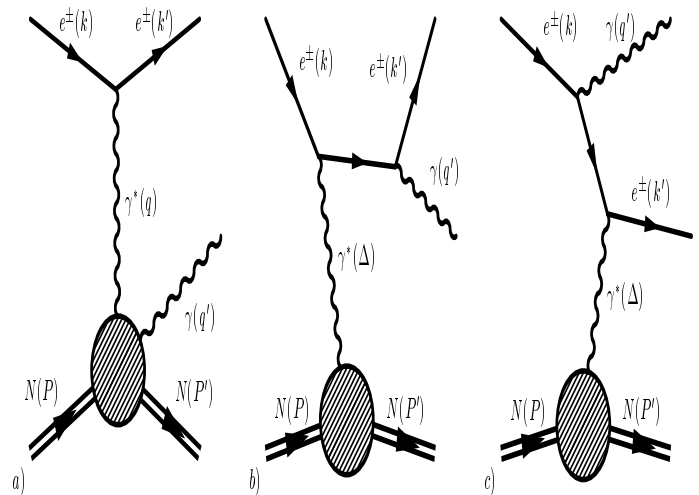


FIG. 1: (Color online) a) DVCS graph, b) BH with photon from final state lepton and c) with photon from initial state lepton.

plitude may extend all the way to the highest  $x_{bj}$  where the coherent peak is still present, that is  $x_{bj} \sim 0.2$ . This is due to a curious interplay between nuclear shadowing and anti-shadowing for  $10^{-2} \leq x_{bj} \leq 10^{-1}$ .

In the second paper we will estimate various DVCS observables. The main focus will be on the kinematic region of the EIC collider, though we will also give numbers for fixed target kinematics. Overall we find that DVCS signals are large enough for all standard observables to be measured with high accuracy at the EIC.

## II. A NUCLEAR GPD MODEL AND NUCLEAR DVCS AMPLITUDES

In the following, we will use and review the model for twist-2 GPDs first introduced in [12] using the off-diagonal representation [15] of GPDs.

Based on the aligned jet model (AJM) (see for example [16]) the key Ansatz of [12] in the DGLAP region is:

$$H^{S,NS,g}(X, \zeta) \equiv \frac{q^{S,NS,g}\left(\frac{X-\zeta/2}{1-\zeta/2}\right)}{1-\zeta/2}, \quad (1)$$

where  $q^i$  refers to any forward distribution and  $H^{S,NS}(X, \zeta) = H^q(X, \zeta) \pm H^{\bar{q}}(X, \zeta)$ . This Ansatz in the DGLAP region corresponds to a double distribution model [17, 18, 19] with an extremal profile function allowing no additional skewness save for the kinematic one.

Note that we choose a GPD representation first introduced in [15], which is maximally close to the inclusive case i.e  $X \in [0, 1]$ ,  $\zeta = x_{bj}$  with the partonic or DGLAP region in  $[\zeta, 1]$  and the distributional amplitude or ERBL region in  $[0, \zeta]$ . Note here that in the case of nuclei we speak of the momentum fractions per nucleon, therefore,  $\zeta \in [0, A]$ .

The prescription in Eq. (1) does not dictate what to do in the ERBL region, which does not have a forward analog. The GPDs have to be continuous through the point  $X = \zeta$  and should have the correct symmetries around the midpoint of the ERBL region. They are also required to satisfy the requirements of polynomiality:

$$\begin{aligned}
M_N &= \int_{\zeta}^1 \frac{dX \tilde{X}^{N-1}}{2-\zeta} \left[ H^g(X, \zeta) - (-1)^{N-1} H^{\bar{q}}(X, \zeta) \right. \\
&\quad \left. + \frac{(1+(-1)^N)}{2} \tilde{X} H^g(X, \zeta) \right] \\
&\quad + (-1)^N \int_0^{\zeta} \frac{dX \tilde{X}^{N-1}}{2-\zeta} \left[ H^{\bar{q}}(X, \zeta) + \tilde{X} H^g(X, \zeta) \right] \\
&= \sum_{k=0}^{N/2} \left( \frac{\zeta}{2-\zeta} \right)^{2k} C_{2k,N}, \tag{2}
\end{aligned}$$

with  $\tilde{X} = \frac{X-\zeta/2}{1-\zeta/2}$ . The ERBL region is therefore modeled with these natural features in mind. One demands that the resultant GPDs reproduce the first moment  $M_1 = 3$  and the second moment  $M_2 = 1 + C\zeta^2/(2-\zeta)^2$  [20].  $C$  was computed in the chiral-quark-soliton model [21] and found to be  $-3.2$  and is related to the D-term [22] which lives exclusively in the ERBL region. This reasoning suggests the following simple analytical form for the ERBL region ( $X < \zeta$ ):

$$\begin{aligned}
H^{g,NS}(X, \zeta) &= H^{g,NS}(\zeta) \left[ 1 + A^{g,NS}(\zeta) C^{g,NS}(X, \zeta) \right], \\
H^S(X, \zeta) &= H^S(\zeta) \left( \frac{X-\zeta/2}{\zeta/2} \right) \left[ 1 + A^S(\zeta) C^S(X, \zeta) \right], \tag{3}
\end{aligned}$$

where the functions

$$\begin{aligned}
C^{g,NS}(X, \zeta) &= \frac{3}{2} \frac{2-\zeta}{\zeta} \left( 1 - \left( \frac{X-\zeta/2}{\zeta/2} \right)^2 \right), \\
C^S(X, \zeta) &= \frac{15}{2} \left( \frac{2-\zeta}{\zeta} \right)^2 \left( 1 - \left( \frac{X-\zeta/2}{\zeta/2} \right)^2 \right), \tag{4}
\end{aligned}$$

vanish at  $X = \zeta$  to guarantee continuity of the GPDs. The  $A^i(\zeta)$  are then calculated for each  $\zeta$  by demanding that the first two moments of the GPDs are explicitly satisfied. For the second moment, what is done in practice is to set the D-term to zero and demand that for each flavor the whole integral over the GPD is equal to the whole integral over the forward input PDF without the shift. For the final GPD, of course, the D-term is added to the quark-singlet (there is no D-term in the non-singlet sector) using the results from the chiral-quark-soliton model [21]. The gluonic D-term, about which nothing is known save its symmetry, is set to zero for  $Q_0$ . Due to the gluon-quark mixing in the singlet channel, there will be a gluonic D-term generated through evolution.

It would be straightforward to extend this algorithm to satisfy polynomiality to arbitrary accuracy by writing the  $A^i(\zeta)$  explicitly as a polynomial in  $\zeta$  where the first

few coefficients are set by the first two moments and the other coefficients are then either determined by the arbitrary functional form, as is done here, or, perhaps theoretically more appealing, one chooses orthogonal polynomials, such as Gegenbauer polynomials, for which one can set the unknown higher moments equal zero. Phenomenologically speaking, the difference between the two choices is negligible.

The above Ansatz also satisfies the required positivity conditions [18, 23, 24] and is in general extremely flexible both in its implementation and adaption to either other forward PDFs or other functional forms in the ERBL region. Therefore, it can be easily incorporated into a fitting procedure making it phenomenologically very useful. Since we will concern ourselves only with NLO, in what follows we will use CTEQ6M [25] as the forward distribution.

In order to extend this parameterization for the proton to a nucleus, we have to include the effects due to the nuclear medium. We do this by multiplying the GPD in Eq. (1) with the ratio of nuclear per nucleon to nucleon inclusive parton distribution function (PDF) shifted by the same amount as the forward distribution in Eq. (1):

$$\frac{1}{A} H_A^{S,NS,g}(X, \zeta) = H^{S,NS,g}(X, \zeta) \cdot \frac{q_A^{S,NS,g} \left( \frac{X-\zeta/2}{1-\zeta/2} \right)}{A \cdot q^{S,NS,g} \left( \frac{X-\zeta/2}{1-\zeta/2} \right)}. \tag{5}$$

The ratio of nuclear to nucleon PDF is taken from [8], [4]. Note that the parametrization of Eq.5 corresponds to the same value of  $M_1$  as for the nucleon (which is anyway necessary to satisfy the baryon charge conservation) and also leads to an A-independent D-term. Note that it is difficult to generate an A-dependent D-term via an attachment of the current to the simplest t-channel exchanges. As an example consider the contribution to the D-term due to two pions or a resonance in the t-channel. The two-pion term where the pions are attached to two different nucleons, is strongly suppressed for large A since it requires a spin flip of both nucleons. Furthermore, it is quite difficult to attach a resonance to two nucleons. At the same time, one cannot exclude the possibility of a coherent interaction of a current with several nucleons. In fact, the real part of the amplitude appears to be more sensitive to large distance effects which may enhance coherent effects. Hence, one cannot exclude that the D-term actually does depend on the atomic number[30]. However, the quantities we consider are not very sensitive to the D-term and so taking the D-term to be independent of A seems to be a natural first approximation.

As far as the  $t$ -dependence is concerned, we postpone the discussion to the next paper dealing with nuclear DVCS observables. Thus we will consider the case  $t = 0$  for the time being. This is sufficient at present, since larger values of  $t \gg t_{min}$  will not be experimentally accessible in the coherent peak we are interested in.

After having evolved the GPDs using the same program successfully employed in [14], the real and imagi-

nary part of the twist-2 DVCS amplitude in LO and NLO given below are calculated using the same program as in [26]:

$$\begin{aligned} \mathcal{A}_{DVCS}^S(\zeta, \mu^2, Q^2) &= \sum_a e_a^2 \left( \frac{2-\zeta}{\zeta} \right) \times \\ &\left[ \int_0^1 dX T^{S_a} \left( \frac{2X}{\zeta} - 1 + i\epsilon, \frac{Q^2}{\mu^2} \right) \mathcal{F}^{S_a}(X, \zeta, \mu^2) \right. \\ &\left. \mp \int_{\zeta}^1 dX T^{S_a} \left( 1 - \frac{2X}{\zeta}, \frac{Q^2}{\mu^2} \right) \mathcal{F}^{S_a}(X, \zeta, \mu^2) \right], \quad (6) \end{aligned}$$

$$\begin{aligned} \mathcal{A}_{DVCS}^g(\zeta, \mu^2, Q^2) &= \frac{1}{N_f} \left( \frac{2-\zeta}{\zeta} \right)^2 \times \\ &\left[ \int_0^1 dX T^g \left( \frac{2X}{\zeta} - 1 + i\epsilon, \frac{Q^2}{\mu^2} \right) \mathcal{F}^g(X, \zeta, \mu^2) \right. \\ &\left. \pm \int_{\zeta}^1 dX T^g \left( 1 - \frac{2X}{\zeta}, \frac{Q^2}{\mu^2} \right) \mathcal{F}^g(X, \zeta, \mu^2) \right], \quad (7) \end{aligned}$$

where  $\mathcal{F}$  stands for the nuclear GPD  $H_A$  and  $\mathcal{A}^i$  for the respective Wilson coefficient functions.

The  $+i\epsilon$  prescription is implemented using the Cauchy principal value prescription (“P.V.”) through the following algorithm:

$$\begin{aligned} P.V. \int_0^1 dX T \left( \frac{2X}{\zeta} - 1 \right) \mathcal{F}(X, \zeta, Q^2) &= \\ \int_0^{\zeta} dX T \left( \frac{2X}{\zeta} - 1 \right) (\mathcal{F}(X, \zeta, Q^2) - \mathcal{F}(\zeta, \zeta, Q^2)) &+ \\ \int_{\zeta}^1 dX T \left( \frac{2X}{\zeta} - 1 \right) (\mathcal{F}(X, \zeta, Q^2) - \mathcal{F}(\zeta, \zeta, Q^2)) & \\ + \mathcal{F}(\zeta, \zeta, Q^2) \int_0^1 dX T \left( \frac{2X}{\zeta} - 1 \right) . & \quad (8) \end{aligned}$$

The relevant LO and NLO coefficient functions are the same as for the nucleon and can be found in [26, 27].

### III. RESULTS FOR NUCLEAR DVCS AMPLITUDES

In the following we give our results for the unpolarized nuclear DVCS amplitudes in NLO for the following nuclei:  $O-16$ ,  $CA-40$ ,  $Pd-110$  and  $Pb-208$ . We will use the FGS [8] and the Eskola et al. [4] parameterizations of nuclear medium effects. The initial scale for the perturbative evolution in both cases will be  $Q_0^2 = 2 \text{ GeV}^2$ . We choose such a low scale to be able to make statements about HERMES kinematics ( $0.05 \leq x_{bj} \leq 0.3$  and  $1 \leq Q^2 \leq 9 \text{ GeV}^2$ ) in our forthcoming paper on nuclear DVCS observables. The FGS parameterization has an initial scale of  $Q_0^2 = 4 \text{ GeV}^2$  and we, therefore, evolve it backward to our  $Q_0$ . The parameterization of Eskola et al. has a  $Q_0^2 = 2.25 \text{ GeV}^2$  and is thus close enough to our

starting scale. Unfortunately, it is a LO parameterization which we will use in NLO.

Our treatments of these two parameterizations can be rightfully called into question. However, our aim at this point is not to make precision statements about nuclear DVCS but rather look for the type of effects which can be expected and how parameterization dependent they are. If the differences in parameterizations will also materialize in DVCS observables in a noticeable way, experiments we will have a good chance of discriminating between different parameterization relying on different assumptions of the underlying physics.

Let us first concentrate on the imaginary part of the unpolarized nuclear DVCS amplitude which depends only on the DGLAP region. In Fig. 2, we show the ratio of the imaginary part of nuclear to nucleon DVCS amplitude in NLO for fixed  $Q^2$  and varying  $x_{bj}$  and in Fig. 3 we show the same ratio for fixed  $x_{bj}$  and varying  $Q^2$ .

As is easily seen from Fig. 2, the nuclear shadowing corrections differ substantially between the two parameterizations at low  $Q^2$  and are very similar for larger  $Q^2$ . However, the nuclear shadowing corrections are in both cases stronger than in the forward case of  $F_2^A/F_2$  (see for example [8]). In particular in the region of small  $x_{bj} \leq 5 \times 10^{-3}$  one observes a significant slope increase in  $x_{bj}$  compared to the forward case. This behavior is easily explained with first the shifted input toward lower values of  $X$ . This leads to enhanced nuclear shadowing in the small  $x_{bj}$  region since shadowing continues to increase toward smaller values of  $x_{bj}$ . Secondly, since the value of the imaginary part of the amplitude is mainly determined by the region  $X \simeq O(\zeta)$  of large light-like distances (see [28]) and since this region is enhanced by perturbative evolution, one expects that until the nuclear enhancement effects from large  $X$  are degraded enough in momentum through evolution, nuclear shadowing effects will increase with the increase in  $Q^2$ . As can be seen from Fig. 3,  $Q^2$  evolution for fixed  $x_{bj}$  will indeed initially increase nuclear shadowing but the vanishing of nuclear shadowing with an increase in  $Q^2$  as seen in  $F_2^A/F_2$  does not happen as rapidly as in DVCS. This occurs precisely because the relevant region for the value of the amplitude is the one of large light-like correlations  $X \simeq O(\zeta)$  which is enhanced through perturbative evolution. Large-light like correlations in turn are more sensitive to nuclear medium effects and thus nuclear shadowing will remain stronger for a wider range in  $Q^2$ . We also observe a stronger  $A$  dependence at small than at large  $x_{bj}$  which is again stronger than the forward case. Once more the shift to relative smaller values of  $x_{bj}$  is the reason. Nuclear shadowing is stronger for  $Pb-206$  than for  $O-16$  and thus a relative shift to smaller values of  $x_{bj}$  will increase this difference further. Evolution does not change this picture a lot since the evolution effects are the same for all nuclei. As we just explained, nuclear shadowing persists under evolution for a wider range in  $Q^2$  than in the forward case where nuclear shadowing disappears more rapidly and hence differences between

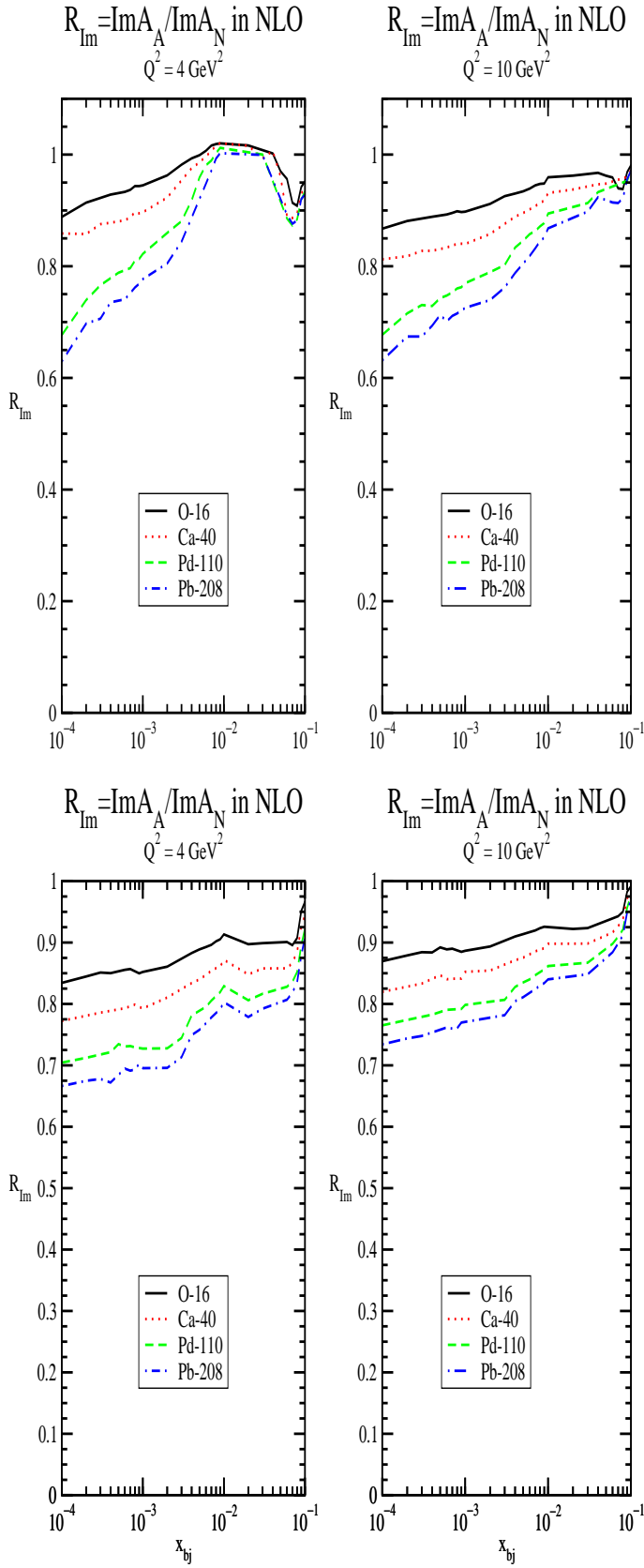


FIG. 2: (Color online) Ratio of nuclear per nucleon to nucleon DVCS amplitudes vs.  $x_{bj}$  for two values of  $Q^2$  for the FGS (upper plot) and Eskola (lower plot) parameterizations.

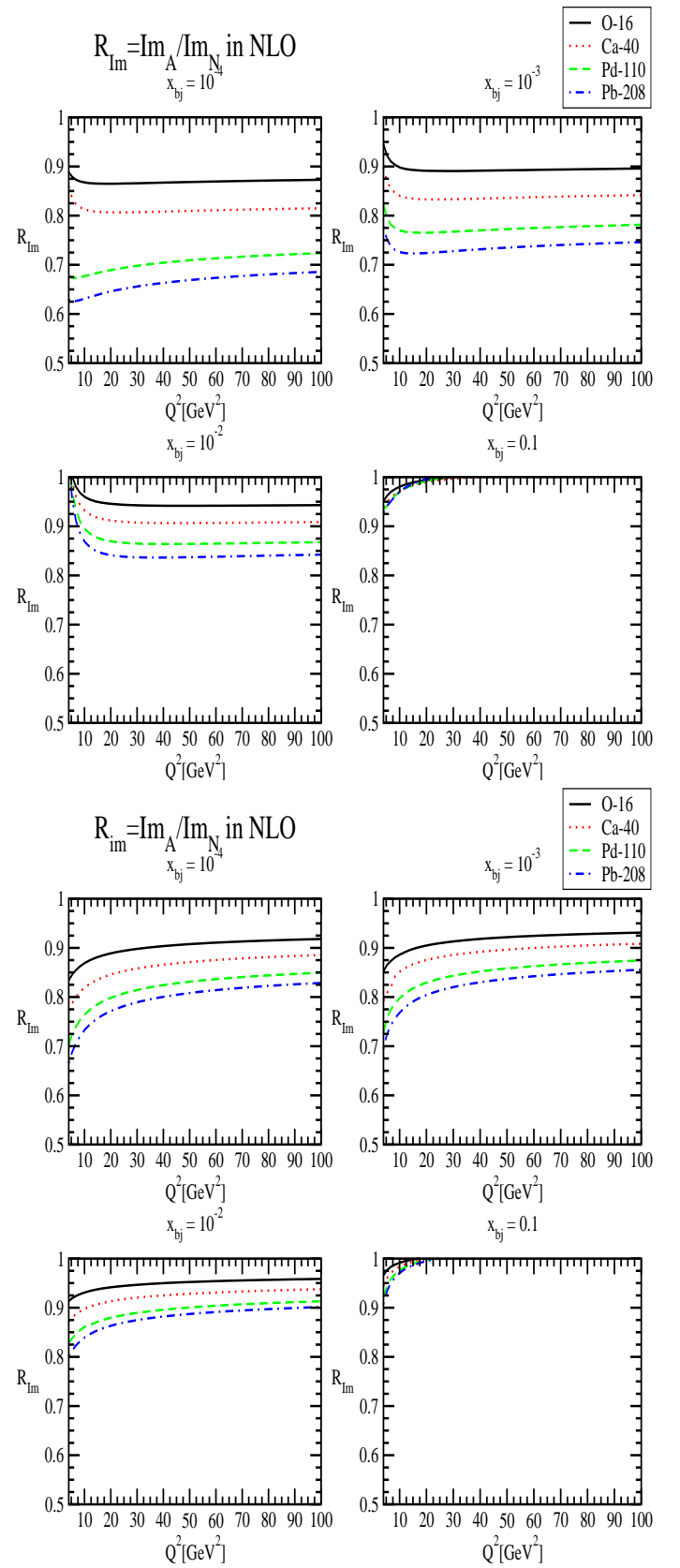


FIG. 3: (Color online) Ratio of nuclear per nucleon to nucleon DVCS amplitudes vs.  $Q^2$  for four values of  $x_{bj}$  for the FGS (upper plot) and Eskola (lower plot) parameterizations.

nuclei as well. When comparing the two parameterizations one notices the peculiar behavior of the ratio for the FGS parameterization at  $Q^2 = 4 \text{ GeV}^2$  in the region of  $5 \times 10^{-3} \leq x_{bj} \leq 10^{-1}$ . This is due to the fact that in the FGS parameterization the ratio of nuclear to nucleon gluon PDF is above 1 in the region  $10^{-2} \leq x_{bj} \leq 10^{-1}$  and we are using shifted distributions as our input for the GPDs. As it turns out the imaginary part of gluon amplitude is negative whereas it is positive for the quarks [26] and the relative suppressions in the quark and the gluon are sufficiently different enough in nuclei and nucleons that in the sum this difference disappears! Note that this is not the case for the Eskola parameterization. However, at  $Q^2 = 10 \text{ GeV}^2$  this behavior has disappeared and the ratio is the same for both distributions within 10 – 15%. The  $A$  dependence of the two parameterizations is quite different at lower  $Q^2$ , however, quite similar at larger  $Q^2$ .

We now turn to the real part of the DVCS amplitude which depends both on the ERBL and the DGLAP region. In Fig. 4, we plot the ratio of the real part of nuclear to nucleon DVCS amplitude in NLO for fixed  $Q^2$  and varying  $x_{bj}$  and in Fig. 3 we show the same ratio for fixed  $x_{bj}$  and varying  $Q^2$ .

As can be readily seen in Fig. 4 the behavior of the real part, for both parameterizations, is substantially different from the one of the imaginary part for both parameterizations except for the smallest values of  $x_{bj}$ . In particular the dip in the ratio in the region  $10^{-2} \leq x_{bj} \leq 10^{-1}$  is very surprising. The reason for this suppression is quite deep. To put it in a nutshell, it is the confluence of the nuclear medium effects: nuclear shadowing at small  $x_{bj}$  and anti-shadowing at large  $x_{bj}$  which mix under evolution. How is that possible?

The real part of the amplitude has two contributions: one originating in the ERBL region and one in the DGLAP region with a relative minus sign between them. If one were to decrease the contribution from the ERBL region and increase the contribution from the DGLAP region, one can obtain a significantly different value from the nucleon with just a relative small change in both contributions due to the relative minus sign. This is precisely what happens. To be definite let us take  $x_{bj} = 5 \times 10^{-2}$ . At this value of  $x_{bj}$  the value of the quark singlet is virtually not shadowed with gluon already experiencing a stronger suppression due to the relative shift to smaller values of  $X$  where nuclear shadowing is stronger. However, due to the nuclear enhancement at larger  $X$ , the quark and gluon distributions in the ERBL are smaller compared to the nucleon case in order to fulfill the first and second moment of the nuclear GPD. At smaller  $x_{bj}$  nuclear shadowing leads to an additional suppression. All of this leads to a smaller value of the contribution to the real part from the ERBL region compared to the nucleon case. The contribution from the DGLAP region increases since the value of the contribution due to the nuclear enhancement increases. Therefore we have the required configuration where the ERBL contribution decreases and the DGLAP one increases. This does not

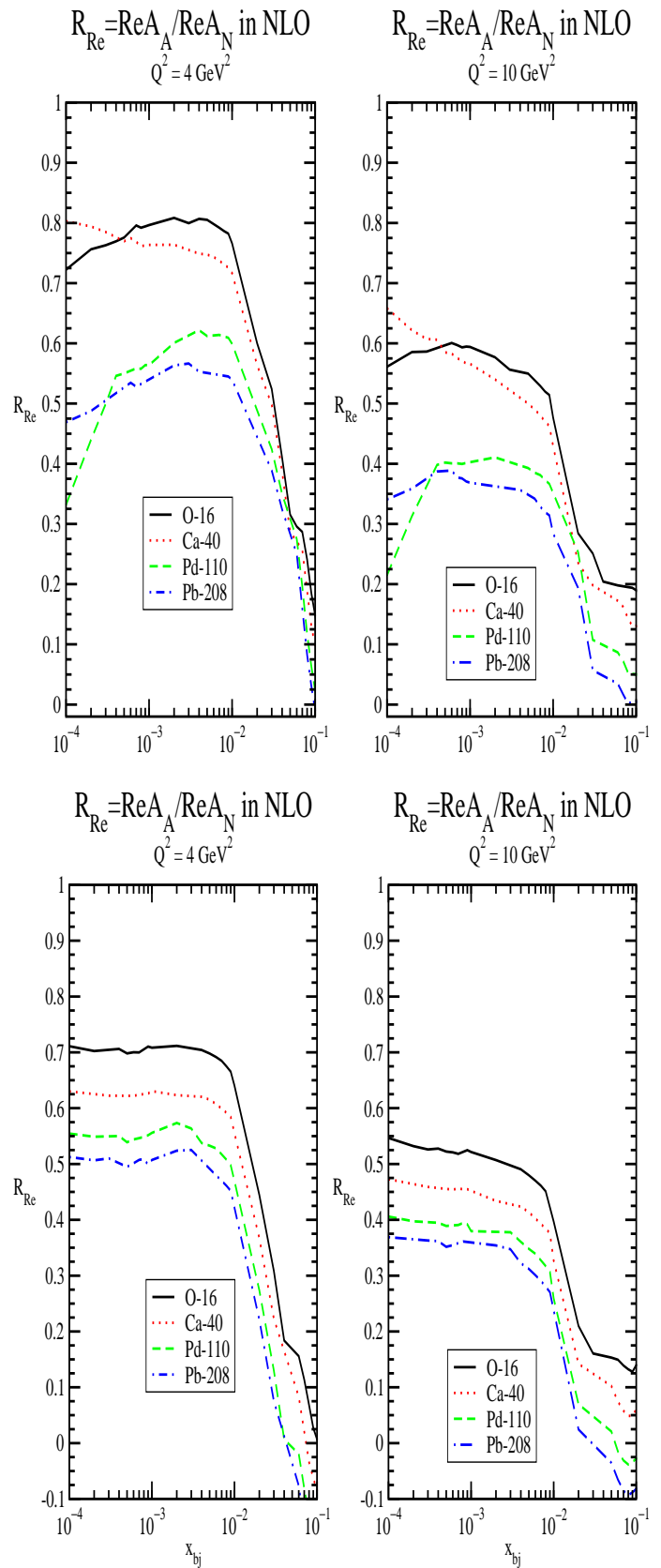


FIG. 4: (Color online) Ratio of nuclear per nucleon to nucleon DVCS amplitudes vs.  $x_{bj}$  for two values of  $Q^2$  for the FGS (upper plot) and Eskola (lower plot) parameterizations.

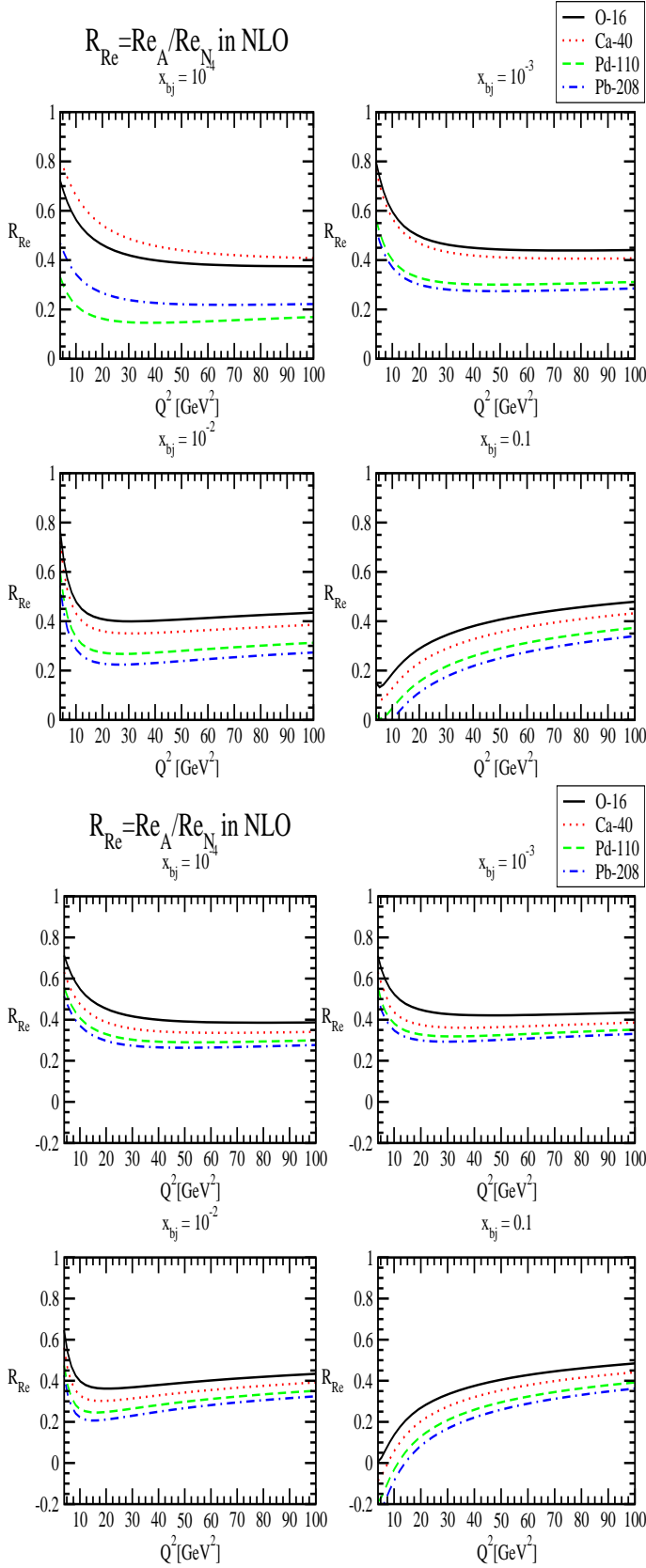


FIG. 5: (Color online) Ratio of nuclear per nucleon to nucleon DVCS amplitudes vs.  $Q^2$  for four values of  $x_{bj}$  for the FGS (upper plot) and Eskola (lower plot) parameterizations.

drastically change under evolution though the nuclear enhancement is pushed into the ERBL region the actual evolution in the ERBL region is slower than in the DGLAP region. Furthermore, the nuclear shadowing in the gluon leads to a slower enhancement of the quark singlet compared to the nucleon case leading basically to a preservation of the effect for a larger range of  $Q^2$  except for the large values of  $x_{bj}$ .

This can be observed in Fig. 5 where the ratio of the real part is plotted vs.  $Q^2$  for fixed  $x_{bj}$  and the suppression effects is seen to decrease slowly at small  $x_{bj}$  and more rapidly at large  $x_{bj}$  though the absolute value of the effect remains large at large  $x_{bj}$  even for large  $Q^2$ . Again, the slow change in the ratio is associated with the predominant enhancement of large light-like distances.

This relative suppression of the ERBL region compared to the nucleon case suggests the simple picture that whereas in the DGLAP region partons could originate in principle from different nuclei, in the ERBL this contribution is strongly suppressed. This once more has to do with the fact that the ERBL region at small  $x_{bj}$  is mainly sensitive to large light-like distances and correlations over large light-like distances are more susceptible to destructive nuclear medium effects leading to a suppression of these parton correlations.

Since the suppression effect is very substantial, it should be clearly measurable in a high precision  $eA$  DVCS experiment at the EIC. We will discuss this in detail in a forthcoming paper.

The above made observations would change somewhat if one were to consider non-zero  $t$  values. If we had performed a comparison at  $t = t_{min} = -x_{bj}^2 m_N^2 / (1 - x_{bj})$  rather than at  $t = 0$  the suppression of the nuclear amplitude at  $x_{bj} \geq 0.01$  would have been even stronger (factor 2 – 5 depending on the considered nucleus) since the nuclear amplitude is suppressed by the nuclear form factor which can be approximated as  $F_A = \exp(R_A^2 t / 6)$  for sufficiently small  $t$ , where  $R_A$  is the electromagnetic radius of the nucleus.

In practical applications considered in [29] the effects of the nuclear form factor for asymmetries are approximately cancelled in the ratio.

Furthermore, for small  $x_{bj}$  nuclear shadowing effects are likely to lead to a small increase of the  $t$ -slope. However, in the case of cross sections integrated over  $t$  (which is the only experimentally measurable quantity) this effect leads to a reduction in the cross section by no more than 10% and it is even smaller for observables sensitive to interference terms.

For  $x_{bj} \gtrsim 0.1 (200/A^{1/3})$  deviations of the  $t$ -dependence from that of the nuclear form factor are much more sensitive to the details of the nuclear dynamics and require a more microscopic treatment than the one presented here. It should be remembered that for  $Pb - 208$   $F_A(t_{min}(x = 0.1))$  is close to the point where the form factor changes sign and thus zero. Therefore, it will be extremely difficult to extract the coherent cross section for such an  $x_{bj}$  even using a veto for production of for-

ward neutrons.

When comparing the two parameterizations one finds a substantial difference at low  $Q^2$  and again similar values at large  $Q^2$  except for the smallest values of  $x_{bj}$  where this difference persists over the entire  $Q^2$  interval. The most curious effect is seen at the smallest values of  $x_{bj}$  for the FGS parameterization where the nuclear medium effect is less for  $CA$  ( $Pb$ ) compared to  $O$  ( $Pd$ ). This is a peculiarity of the parameterization and once more the extreme sensitivity of DVCS to the gluon distribution at small  $x_{bj}$ . Note that the Eskola parameterization does not have this feature since the gluon at small  $x_{bj}$  is substantially different from the FGS parameterization. Experiments will hopefully be able to distinguish this effect in an observable sensitive to the real part like the beam charge asymmetry.

#### IV. CONCLUSIONS

In this paper we propose a model for nuclear GPDs based on the very successful GPD parameterization used in [12] which describes all available world data of DVCS

on the nucleon. We calculate the nuclear DVCS amplitudes using two different parameterizations for the nuclear effects as proposed by [8] and [4] and plot the ratio of nuclear to nucleon DVCS amplitude for both the real and imaginary part. We find an enhancement of nuclear shadowing in the imaginary part for small  $x_{bj}$  compared to the inclusive case which can be traced back to the high sensitivity of DVCS to large light-like correlation distances which can be more easily influenced by nuclear medium effects. In the real part we observe for the first time an interplay between large and small  $x_{bj}$  nuclear effects in hadronic amplitudes for a large range in  $Q^2$ . This interplay is most visible for  $10^{-2} \leq x_{bj} \leq 10^{-1}$  where the effect is strongest and should be observable in an  $eA$  DVCS experiment as for example at the EIC.

#### Acknowledgment

This work was supported by the DFG under the Emmy-Noether grant FR-1524/1-3 and the DOE under grant number DE-FG02-93ER40771.

- 
- [1] L. L. Frankfurt, M. I. Strikman and S. Liuti, Phys. Rev. Lett. **65**, 1725 (1990).
  - [2] K. J. Eskola, Nucl. Phys. B **400**, 240 (1993).
  - [3] T. Gousset and H. J. Pirner, Phys. Lett. B **375**, 349 (1996) [arXiv:hep-ph/9601242].
  - [4] K.J. Eskola, V.J. Kolhinen and P.V. Ruuskanen, Nucl. Phys. B **535** (1998) 351; K.J. Eskola, V.J. Kolhinen and C.A. Salgado, Eur. Phys. J. C **9** (1999) 61.
  - [5] G. Piller, W. Ratzka and W. Weise, Z. Phys. A **352** (1995) 427.
  - [6] W. Melnitchouk and A.W. Thomas, Phys. Rev. D **47** (1993) 3783; Phys. Lett. B **317** (1993) 437; Phys. Rev. C **52** (1995) 3373; *Nuclear shadowing at low  $Q^{2*}$* , hep-ex/0208016.
  - [7] A. Capella, A. Kaidalov, C. Merino, D. Pertermann and J. Tran Thanh Van, Eur. Phys. J. C **5** (1998) 111.
  - [8] L. Frankfurt, V. Guzey and M. Strikman, arXiv:hep-ph/0303022.
  - [9] L. Frankfurt and M. Strikman, Eur. Phys. J. A **5** (1999) 293.
  - [10] L. Frankfurt, V. Guzey, M. McDermott and M. Strikman, J. High Energy Phys. **202** (2002) 27.
  - [11] V. Guzey and M. Strikman, Phys. Rev. C **68**, 015204 (2003).
  - [12] A. Freund, M. McDermott and M. Strikman, Phys. Rev. D **67**, 036001 (2003).
  - [13] H1 Collaboration, C. Adloff *et al.*, Phys. Lett. B **517**, 47 (2001), ZEUS Collaboration, P. R. Saull, hep-ex/0003030, ZEUS Collaboration, hep-ex/0305028, HERMES Collaboration, Phys. Rev. Lett. **87**, 182001(2001), HERMES Collaboration, Nucl. Phys. A **711**, 171 (2002), CLAS Collaboration, S. Stepanyan *et al.*, Phys. Rev. Lett. **87**, 182002 (2001).
  - [14] A. Freund and M. McDermott, Phys. Rev. D **65**, 074008 (2002).
  - [15] K. J. Golec-Biernat and A. D. Martin, Phys. Rev. D **59**, 014029 (1999).
  - [16] L. Frankfurt and M. Strikman, Phys. Rept. **160**, 235 (1988); Nucl. Phys. B **316**, 340 (1989).
  - [17] A. V. Radyushkin, Phys. Rev. D **56**, 5524 (1997).
  - [18] A. V. Radyushkin, Phys. Rev. D **59**, 014030 (1999).
  - [19] A. V. Radyushkin, Phys. Lett. B **449**, 81 (1999).
  - [20] The first moment counts the number of quarks in the proton and the second moment is a generalization of the momentum sum rule where the D-term generates all the deviation from unity as  $\zeta$  varies.
  - [21] N. Kivel, M. V. Polyakov and M. Vanderhaeghen, Phys. Rev. D **63**, 114014 (2001).
  - [22] M. V. Polyakov and C. Weiss, Phys. Rev. D **60**, 114017 (1999).
  - [23] B. Pire, J. Soffer and O. Teryaev, Eur. Phys. J. C **8**, 103 (1999).
  - [24] P. V. Pobylitsa, hep-ph/0211160, Phys. Rev. D **67**
  - [25] J. Pumplin *et al.*, CTEQ Collaboration, J. High Energy Phys. **0207**, 012 (2002).
  - [26] A. Freund and M. McDermott, Phys. Rev. D **65**, 056012 (2002).
  - [27] A. V. Belitsky *et al.*, Nucl. Phys. B **593**, 289 (2001).
  - [28] A. Freund, Eur. Phys. J. C **31**, 203 (2003).
  - [29] A. Freund and M. Strikman, hep-ph/0309065.
  - [30] We thank M.Polyakov for a discussion of this point